Structure-activity relation of Re nanoparticles

Payam Kaghazchi* and Timo Jacob
Institute of Electrochemistry, Ulm University, Albert-Einstein-Allee 47, D-89069 Ulm, Germany
(Received 23 May 2012; published 20 August 2012)

By combining density functional theory and thermodynamic considerations we determined the equilibrium shape of Re particles in contact with O_2 and N_2 environments. At low and intermediate coverages oxygen adsorption has a minor influence on the particle shape, while nitrogen adsorption leads to the stabilization of spherically shaped polyhedra with a large contribution from atomically rough faces. At very high coverages of O and N particles are perfect prisms consisting of low-index faces. By comparing these results with the experimental data for the activity of different Re surfaces we propose that the experimentally measured high initial activity of polycrystalline Re for ammonia synthesis might be due to the N-induced formation of high-index faces with a high density of low-coordinated atoms (roughening). Moreover, the measured decrease in the activity of polycrystalline Re at saturation coverage might be because of the N-induced formation of close-packed faces (smoothing). Our calculations suggest that adsorbate-induced roughening or smoothing of catalytic particles on the atomic scale is capable of controlling the activity of the catalysts.

DOI: 10.1103/PhysRevB.86.085434 PACS number(s): 61.46.Df

I. INTRODUCTION

Catalysts are used in many industrial processes. Hence a major scientific challenge for the 21st century is to achieve a high degree of reactivity and selectivity of industrial catalysts, which usually consist of high-surface area nanoparticles (NPs) on a support material.

The performance of a catalyst depends strongly on shape and size of the NP. For instance, in most cases smaller NPs are found to be more active [e.g., CO oxidation over Cu and Ag NPs,[1,2] and NO[3] or CO_2 reduction as well as CO hydrogenation over Au NPs[4]]. Here it is argued that the ratio between the surface area and particle volume and the overall density of low-coordinated sites, which increases as the size of a particle decreases, might be responsible.[5]

There are relatively few studies on the shape-activity relation of NPs. Tian *et al*. have found that tetrahexahedral (THH) Pt NPs are more active (up to 400%) for the electrooxidation of formic acid and ethanol compared to other (equivalent surface area) shapes.[6] The higher activity of THH NPs was attributed to their high-index faces [i.e., Pt(210), (520), (730)] that are expected to be more active than close-packed faces.[6] Further, it was demonstrated that the THH NPs are chemically stable since their shape remained unchanged during the reaction.[6]

However, the equilibrium shape (ES) of NPs, which is usually given by a Wulff construction,[7] might change drastically with environmental conditions. This is due to the fact that the ES is determined by the anisotropy in surface free energies (SFE) of different faces, which can be modified by adsorbates. For example, although density functional theory (DFT) calculations have shown that the ES of clean Ru NPs is a polyhedron consisting of $\{0001\}$, $\{10\bar{1}0\}$, and $\{11\bar{2}1\}$ faces together with small contributions of $\{10\bar{1}2\}$ and $\{11\bar{2}0\}$ faces,[8] experimental measurements demonstrate that the higher-index $\{11\bar{2}1\}$ and $\{10\bar{1}2\}$ faces disappear in the presence of alkylamine since $\{10\bar{1}1\}$ faces are formed at their expense.[9] Therefore, the performance of NPs can depend strongly on their chemical environment due to adsorbate-induced shape changes.

First-principles studies of adsorbate-induced changes of the NP shapes are computationally demanding since knowledge about the stability of various surface orientations as a function of adsorbate-coverage is required. Low-index surfaces are generally the most stable structures and therefore are expected to be present on the NPs. In the presence of strongly interacting adsorbate (i.e., O, N, or Cl), the close-packed surfaces are still expected to be favorable while higher-index surfaces are usually unstable and facet into more stable surfaces. Therefore, low-index surfaces are also expected to be the probable faces of adsorbate-covered NPs.

Although several works have been devoted to determine the ES of mainly fcc-structured NPs of pure metals[10,11] and metal oxides[12,13] in the presence of adsorbates, much less attention has been paid to hcp-structured ones such as Re, which are known to be very active for ammonia synthesis and oxidation reactions.[14,15] Recently, we have studied the morphology of Re surfaces in contact with gaseous O_2 and N_2. Adsorption of these strongly interacting atoms is important for understanding the primary processes of many important reactions on Re such as ammonia synthesis, selective oxidation of methanol, thiophene, and hydrodesulfurization.[16–21] In the present work, we study the ES of Re particles in contact either with O_2 or N_2. By combining DFT and thermodynamic considerations we obtain the surface energies of O- and N-covered Re surfaces, which are then used to determine the ES by means of a Wulff construction. Comparing our results with previous experimental measurements indicates that adsorbate-induced roughening or smoothing of particles on the atomic scale can play a vital role in understanding or tuning their catalytic activities.

II. METHOD

The important quantity for thermodynamical studies of particle shapes is the overall formation energy, which mainly includes contributions from surfaces, edges, corners, and strain. However, for large particles (usually >3–5 nm) the overall formation energy is dominated by surface contributions while all other energy parts are comparably small. Under this

condition, Wulff's theorem[7] can be adopted to determine the ES in the presence of a gas phase. This theorem states that particles of a given volume are bound with planes of minimum total surface free energy expressed as

$$\min \sum_i \gamma_i(T, p_{\text{gas}}) A_i, \tag{1}$$

where γ_i and A_i are SFE and the area of the ith face, respectively, while T is the temperature and p_{gas} the partial pressure of the surrounding gas.

To evaluate the SFEs we use the *ab initio* atomistic thermodynamics approach[22–25] that allows the stability of surfaces being in contact with a surrounding gas atmosphere (reservoir) characterized by chemical potential or p_{gas} and T to be calculated by *ab initio* methods.

In the present work, the *ab initio* calculations were performed using the DFT code CASTEP[26] with a plane-wave basis set ($E_{\text{cutoff}} = 380$ eV), Vanderbilt ultrasoft pseudopotentials,[27] and the Perdew-Burke-Ernzerhof–generalized gradient approximation (PBE-GGA) exchange-correlation functional.[28] The Brillouin zones of the (1×1)-surface unit cells of Re(0001), $(10\bar{1}0)$, $(10\bar{1}1)$, $(11\bar{2}1)$, and $(13\bar{4}2)$ were sampled with (8×8), (5×8), (4×8), (4×4), and (3×3) Monkhorst-Pack **k**-point meshes. The surfaces were modeled by 5-, 11-, 14-, 19-, and 30-layer slabs, respectively, separated by at least 13 Å vacuum. The bottom 2, 4, 4, 4, and 14 layers were fixed at the calculated bulk structure, and the geometry of the remaining layers was fully optimized (up to <0.03 eV/Å).

III. RESULTS AND DISCUSSION

We carried out extensive DFT calculations on low-index Re(0001), $(10\bar{1}0)$, $(10\bar{1}1)$, and $(11\bar{2}1)$, which are expected to be among the most stable structures, as well as high-index Re$(13\bar{4}2)$ surfaces that were found to be stable in O- and N-induced surface faceting of rhenium.[29–31]

The total energies obtained for the most favorable structures of the clean as well as O- and N-covered Re surfaces have then been used to evaluate the corresponding SFEs using the *ab initio* atomistic thermodynamics approach. The resulting diagrams, where the SFEs of clean as well as O- and N-covered Re(0001), $(10\bar{1}0)$, $(10\bar{1}1)$, $(11\bar{2}1)$, and $(13\bar{4}2)$ surfaces are plotted as a function of the chemical potential of the surrounding oxygen and nitrogen atmosphere (referenced by $\Delta\mu_{\text{O}} = \mu_{\text{O}} - \frac{1}{2}E^{\text{tot}}_{\text{O}_2}$ and $\Delta\mu_{\text{N}} = \mu_{\text{N}} - \frac{1}{2}E^{\text{tot}}_{\text{N}_2}$), are shown in Fig. 1. Only those phases (lines) are shown which are most stable (lowest lying) in their particular O and N chemical potential range. For each surface, below a critical $\Delta\mu_{\text{O}}$ ($\Delta\mu_{\text{N}}$), where no oxygen (nitrogen) is adsorbed on the surface, the stability does not change (horizontal lines). Above this critical O (N) chemical potential, O (N) atoms start binding to the surface (nonhorizontal lines), while the O (N) coverage on the surface increases gradually with $\Delta\mu_{\text{O}}$ ($\Delta\mu_{\text{N}}$) (the higher the coverage, the steeper the slope). Since we are only interested in adsorption on pure Re surfaces, we excluded the high chemical potential ranges where Re bulk oxides or nitrides are expected to become thermodynamically stable. In the present work, we did not study the absorption of O into subsurface sites since there is no experimental evidence for the formation of these structures under conditions where no bulk oxide is formed [for example, see Ref. 32 on O/$(10\bar{1}0)$]. Similarly, we have not studied surface-nitride structures since a stable bulk Re-nitride cannot be obtained directly from the elements of Re and N.[33] However, we have considered the experimentally observed O-induced reconstructions on low-index surfaces: missing-row Re$(10\bar{1}0)$-(1×3)[32,34] and missing-row Re$(10\bar{1}1)$-(1×2).[35] We find that the Re$(10\bar{1}0)$ and $(10\bar{1}1)$ faces of NPs that are discussed in the following are unreconstructed.

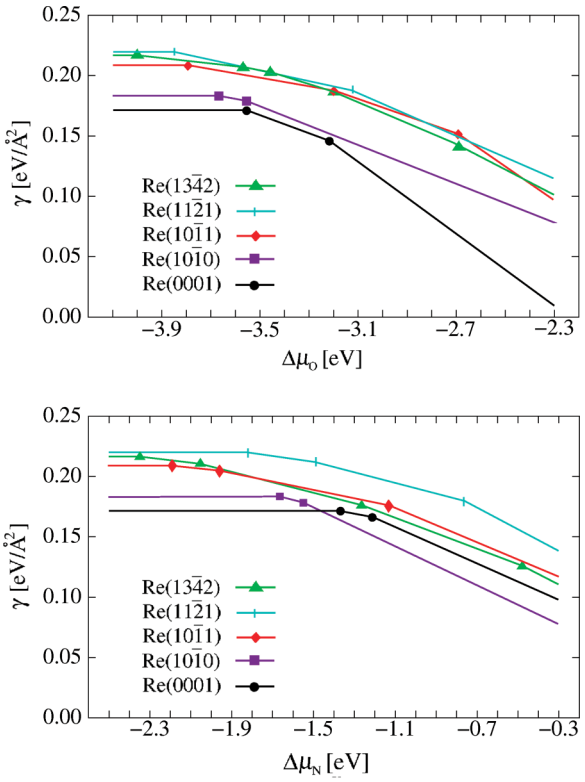

FIG. 1. (Color online) Surface phase diagram for O/Re (top panel) and N/Re (bottom panel) surfaces showing the surface free energy a as function of the O and N chemical potential referenced as $\Delta\mu_{\text{O}} = \mu_{\text{O}} - \frac{1}{2}E^{\text{tot}}_{\text{O}_2}$ and $\Delta\mu_{\text{N}} = \mu_{\text{N}} - \frac{1}{2}E^{\text{tot}}_{\text{N}_2}$.

Based on the surface phase diagrams we constructed the Wulff shapes of O/Re and N/Re particles satisfying Eq. (1) as a function of $\Delta\mu_{\text{O}}$ and $\Delta\mu_{\text{N}}$ (see Fig. 2). To compare to experimental coverages (i.e., physical monolayers) we assumed the highest possible O/N coverage from our calculated phase diagrams (prior to forming the bulk oxides or nitrides, respectively) to correspond to 1 ML (saturation).

We find that without adsorption ($\Delta\mu_{\text{O}} \leqslant -4.30$ eV or $\Delta\mu_{\text{N}} \leqslant -2.35$ eV) the ES is a polyhedron, whose dominating faces are low index (0001), $(10\bar{1}0)$, and $(10\bar{1}1)$. This is due to the lower SFEs of these surfaces compared to the high-index $(11\bar{2}1)$ and $(13\bar{4}2)$ ones, as can be seen in Fig. 1.

Changes in the overall morphology and the shape of the NPs are related to the adsorbate-dependent anisotropy of the SFEs of different surface orientations. At low coverages of O ($\Theta = 0.451$ ML, $\Delta\mu_{\text{O}} \leqslant -3.50$ eV) the relative stability of different faces remains almost unchanged [see Fig. 1(a)] and therefore the ES does not deviate much from that of clean NPs (i.e., polyhedra). However, at higher coverages ($\Theta = 0.498$ ML,

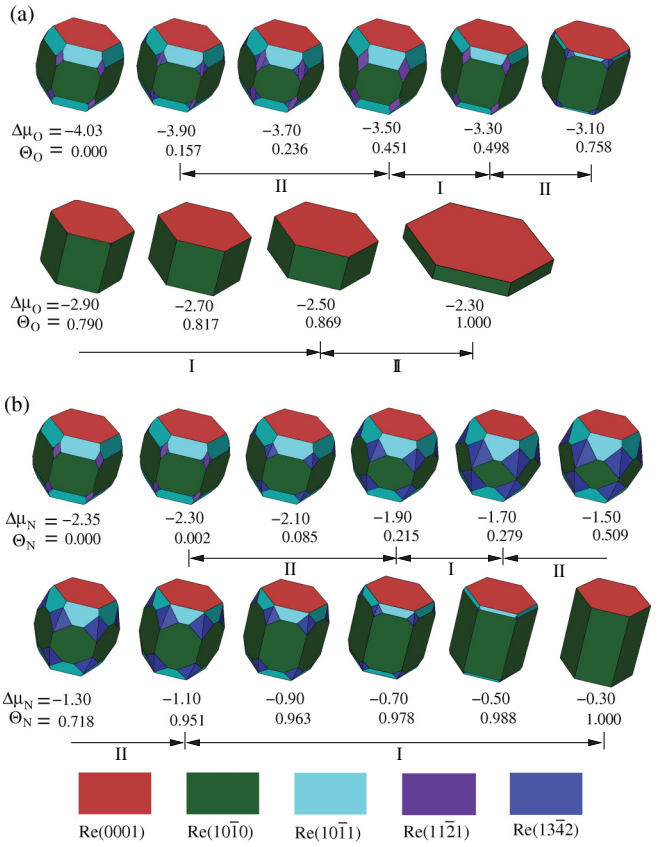

FIG. 2. (Color online) Equilibrium shape (ES) of Re particles as function of (a) oxygen chemical potential $\Delta\mu_O$(eV) and (b) nitrogen chemical potential $\Delta\mu_N$(eV). Only those chemical potential ranges are shown where clean and adsorbate-covered surfaces are formed rather than bulk-oxide or bulk-nitride structures. The calculated O and N coverages (Θ_O and Θ_N) for different chemical potentials are in monolayers ML, where 1 ML corresponds to the estimated saturation coverage. The chemical potential ranges at which the coverage changes a little or a lot have been denoted by I or II, respectively.

$\Delta\mu_O = -3.30$ eV) the preference of (0001) and (10$\bar{1}$0) over other orientations becomes more dominant [see Fig. 1(a)] and therefore the particle's morphology transforms from the polyhedron to an almost prismatic shape, which mainly consists of (0001) and (10$\bar{1}$0) faces. A further increase in $\Delta\mu_O$ (i.e., coverage) causes the stability of (0001) to become increasingly favorable compared to other faces [see Fig. 1(a)], leading to the suppression of (10$\bar{1}$1), (11$\bar{2}$1), and (13$\bar{4}$2) faces and the formation of perfect hexagonal prisms. The preference of (0001) over (10$\bar{1}$0) increases rapidly with $\Delta\mu_O$. Thus, at very high oxygen chemical potentials of -2.30 eV (i.e., at saturation coverage), a thin hexagonal prism represents the ES.

Nitrogen adsorption preferentially stabilizes (13$\bar{4}$2) faces at the expense of (11$\bar{2}$1) ones. This can be seen from Fig. 1(b), where the (11$\bar{2}$1) faces shrink as soon as N adsorption takes place at $\Delta\mu_N = -2.30$ eV and disappear completely at $\Delta\mu_N \geqslant -2.10$ eV. This is in agreement with the experimental studies by Wang *et al.*,[35] showing the stabilization of two-sided ridges, combining (13$\bar{4}$2) and (31$\bar{4}$2) faces, on the planar (11$\bar{2}$1) surface after N adsorption. The partial contribution of the (13$\bar{4}$2) faces to the overall particle surface is determined by the relative stability of this face and its neighbors [i.e., (10$\bar{1}$0) and (10$\bar{1}$1)]. At -1.7 eV $\leqslant \Delta\mu_N \leqslant -1.5$ eV, the (13$\bar{4}$2) face is only ∼12 meV less stable than (10$\bar{1}$0) and is as stable as (10$\bar{1}$1) [see Fig. 1(b)], resulting in a significant contribution of this face to the overall particle's surface. For higher values of $\Delta\mu_N$, the surface free energy of (10$\bar{1}$0) decreases more rapidly than the stability of the other orientations [see Fig. 1(b)]. As a consequence, the (13$\bar{4}$2) and (10$\bar{1}$1) faces disappear gradually. Finally, at $\Delta\mu_N = -0.30$ eV we have a perfect hexagonal prism formed by (0001) and (10$\bar{1}$0) faces. Since the stability of N/Re(10$\bar{1}$0) is larger than N/Re(0001), the height of the hexagonal prism is larger than its diameter, which is opposite to the case of O/Re. This is due to the stabilization of different O and N structures on (10$\bar{1}$0): For N adsorption, we found a zigzag arrangement of N on the Re(10$\bar{1}$0) surface.[34] Interestingly, such an overlayer, which has also been observed for O/Ru(10$\bar{1}$0),[36] does not form for O/Re(10$\bar{1}$0).[34]

The morphology of nanoparticles is one of the key factors responsible for their catalytic behavior. In the present work, we focus on ammonia synthesis on Re, being among the best catalysts for this reaction.[37] To elucidate the structure-activity relation of Re NP catalysts one has to determine the reaction mechanism and barriers on different Re faces. This is computationally very demanding because of the complexity of interactions and reaction paths. Here, we make use of the experimental data reported in the literature on the activity of various Re surfaces towards ammonia synthesis. This enables us to rationalize the experimentally observed coverage-dependent activity of polycrystalline Re for this reaction.

The measured activity ratio of 1:94:920:2820 for Re(0001), (10$\bar{1}$0), (11$\bar{2}$0), and (11$\bar{2}$1) single crystal surfaces indicates a strong structure sensitivity for ammonia synthesis over rhenium.[21] The higher activity of high-index surfaces is possibly due to the existence of low-coordinated binding sites on these surfaces, which can be considered rather active for the activation of N.[14] We have recently shown that Re(11$\bar{2}$1) is not a stable surface after adsorption of N, which is an important step in ammonia synthesis, and readily forms Re(13$\bar{4}$2) facets.[29] Therefore, the high activity of Re(11$\bar{2}$1) towards ammonia synthesis is most likely due to the formation of atomically rough Re(13$\bar{4}$2) surfaces. These surfaces resemble (10$\bar{1}$1) terraces with a high density of steps and kinks, providing low-coordinated binding sites. For this reason, we propose a high activity of Re particles for ammonia synthesis (and possibly other N-involved reactions) for a wide range of N chemical potentials of -2.10 eV $\leqslant \Delta\mu_N \leqslant -0.70$ eV, where a large contribution of (13$\bar{4}$2) faces exists [see Fig. 2(b)]. This N-induced roughening of rhenium NPs on the atomic scale might explain the experimental measurements showing a very high initial activity of polycrystalline Re for the synthesis of ammonia from H and N.[37] One can also understand why the activity of this system decreases for higher background pressures of ammonia (above 1–2 Torr).[37] While this behavior was attributed to "product poisoning" of the catalyst surface by the synthesized ammonia,[37] our calculations show that this might well be due to atomic smoothing of Re particles: For

very high N chemical potentials (-0.70 eV $\leqslant \Delta\mu_N$) the ESs become perfect prisms exposing low-index surface faces [i.e., (0001) and $(10\bar{1}0)$], which are the least active surfaces for ammonia synthesis.[21] For the same reason, we predict that the activity of O-involved reactions on the Re particle decreases with coverage.

IV. CONCLUSION

In summary, on the basis of DFT-based thermodynamics the equilibrium shape of Re particles in the presence of interacting O and N adsorbates was determined. The shape of Re particles with low coverages of O and N is very similar to that of the clean particles. At medium coverages, for O adsorption the contribution of low-index surfaces becomes larger and therefore the ES changes slightly from polyhedral to the almost prismatic shape, while for N adsorption the similar stability of different orientations leads to the stabilization of more spherical-like polyhedra, consisting of both low- and high-index surfaces. Finally, for high coverages of O and N perfect prisms with the lowest-index surfaces are formed. By combining these results with the experimental data for the activity of different Re surfaces we propose that the measured high initial activity of polycrystalline Re for ammonia synthesis might be due to the N-induced roughening on the atomic scale (larger contribution of open surfaces). Moreover, the measured decrease in the activity of polycrystalline Re at saturation coverage might well be because of the N-induced smoothing on the atomic scale (larger contribution of close-packed surfaces). We also predict a decrease in the activity of polycrystalline Re for oxidation reactions at high O coverages.

Our studies suggest that the reactant-induced restructuring of nanoparticular catalysts does indeed lead to dramatic changes in the activity. Further, we expect a similar behavior to be at play for other hcp crystals (i.e., hcp-Ru and hcp-Os), which are also among the rather active catalysts for ammonia synthesis.

ACKNOWLEDGMENTS

The authors gratefully acknowledge support from the "Bundesministerium für Bildung und Forschung" (BMBF) and "Deutsche Forschungsgemeinschaft" (DFG) as well as by the bw grid for computing resources.[38] Further, support by the European Union through the Marie Curie Initial Training Network ELCAT, Proposal No. 214936-2, and the ERC Starting-Grant THEOFUN is acknowledged.

*payam.kaghazchi@uni-ulm.de

[1] M. Lippits, A. Gluhoi, and B. Nieuwenhuys, Top. Catal. **44**, 159 (2007).
[2] N. Lopez, T. V. W. Janssens, B. S. Clausen, Y. Xu, M. Mavrikakis, T. Bligaard, and J. K. Nørskov, J. Catal. **223**, 232 (2004).
[3] A. Ueda and M. Haruta, Gold Bull. **32**, 3 (1999).
[4] H. Sakurai and M. Haruta, Appl. Catal., A **127**, 93 (1995).
[5] B. Roldan Cuenya, Thin Solid Films **518**, 3127 (2010).
[6] N. Tian, Z.-Y. Zhou, S.-G. Sun, Y. Ding, and Z. L. Wang, Science **316**, 732 (2007).
[7] G. Wulff, Z. Kristallogr. **34**, 449 (1901).
[8] J. Aßmann, D. Crihan, M. Knapp, E. Lundgren, E. Löffler, M. Muhler, V. Narkhede, H. Over, M. Schmid, A. P. Seitsonen, and P. Varga, Angew. Chem. Int. Ed. **44**, 917 (2005).
[9] M. V. Brink, M. A. Peck, K. L. More, and J. D. Hoefelmeyer, J. Phys. Chem. C **112**, 12122 (2008).
[10] A. Soon, L. Wong, B. Delley, and S. Catherine, Phys. Rev. B **77**, 125423 (2008).
[11] F. Mittendorfer, N. Seriani, O. Dubay, and G. Kresse, Phys. Rev. B **76**, 233413 (2007).
[12] A. S. Barnard, P. Zapol, and L. A. Curtiss, J. Chem. Theory Comput. **1**, 107 (2005).
[13] A. S. Barnard and L. A. Curtiss, Nano Lett. **5**, 1261 (2005).
[14] G. Haase and M. Asscher, Surf. Sci. **191**, 75 (1987).
[15] Y. Wang and K. Jacobi, J. Phys. Chem. B **108**, 14726 (2004).
[16] I. E. Wachs, G. Deo, A. Andreini, M. A. Vuurman, and M. de Boer, J. Catal. **160**, 322 (1996).
[17] Y. Z. Yuan, T. Shido, and Y. Iwasawa, Chem. Comm. **15**, 1421 (2000).
[18] J. Liu, E. Zhan, W. Cai, J. Li, and W. Shen, Catal. Lett. **120**, 274 (2008).
[19] M. E. Bussell, A. J. Gellman, and G. A. Somorjai, J. Catal. **110**, 423 (1988).
[20] R. Kojima, H. Enomoto, M. Muhler, and K. Aika, Appl. Catal. A **246**, 311 (2003).
[21] M. Asscher, J. Carrazza, M. M. Khan, K. B. Lewis, and G. A. Somorjai, J. Catal. **98**, 277 (1986).
[22] E. Kaxiras, Y. Bar-Yam, J. D. Joannopoulos, and K. C. Pandey, Phys. Rev. B **35**, 9625 (1987).
[23] M. Scheffler, *Physics of Solid Surfaces* (Elsevier, Amsterdam, 1987).
[24] G.-X. Qian, R. M. Martin, and D. J. Chadi, Phys. Rev. B **38**, 7649 (1988).
[25] K. Reuter and M. Scheffler, Phys. Rev. B **65**, 035406 (2002).
[26] M. D. Segall, P. J. D. Lindan, M. J. Probert, C. J. Pickard, P. J. Hasnip, S. J. Clark, and M. C. Payne, J. Phys.: Condens. Matter **14**, 2717 (2002).
[27] D. Vanderbilt, Phys. Rev. B **41**, 7892 (1990).
[28] J. P. Perdew, K. Burke, and M. Ernzerhof, Phys. Rev. Lett. **88**, 3865 (1996).
[29] T. E. Madey, W. Chen, H. Wang, P. Kaghazchi, and T. Jacob, Chem. Soc. Rev. **37**, 2310 (2008).
[30] P. Kaghazchi, T. Jacob, H. Wang, W. Chen, and T. E. Madey, Phys. Rev. B **79**, 132107 (2009).
[31] P. Kaghazchi and T. Jacob, Phys. Rev. B **82**, 165448 (2010).
[32] J. Lenz, P. Rech, K. Christmann, M. Neuber, C. Zubragel, and E. Schwarz, Surf. Sci. **269–270**, 410 (1992).
[33] P. Clark, B. Dhandapani, and S. Oyama, Appl. Catal. A **184**, 175 (1999).
[34] P. Kaghazchi and T. Jacob, Phys. Rev. B **81**, 075431 (2010).
[35] H. Wang, Ph.D. thesis, Rutgers University, 2008.

[36]S. Schwegmann, A. P. Seitsonen, V. De Renzi, H. Dietrich, H. Bludau, M. Gierer, H. Over, K. Jacobi, M. Scheffler, and G. Ertl, Phys. Rev. B **57**, 15487 (1998).

[37]N. D. Spencer and G. A. Somorjai, J. Phys. Chem. **86**, 3493 (1982).

[38]http://www.bw-grid.de, member of the German D-Grid initiative, funded by the Ministry for Education and Research (Bundesministerium fuer Bildung und Forschung) and the Ministry for Science, Research and Arts Baden-Wuerttemberg (Ministerium fuer Wissenschaft, Forschung und Kunst Baden-Wuerttemberg).